Earth and Planetary Science Letters 374 (2013) 227–238

Contents lists available at SciVerse ScienceDirect

Earth and Planetary Science Letters

journal homepage: www.elsevier.com/locate/epsl

# A middle Miocene relative paleointensity record from the Equatorial Pacific

Christian Ohneiser [a,*], Gary Acton [b], James E.T. Channell [c], Gary S. Wilson [a,d], Yuhji Yamamoto [e], Toshi Yamazaki [f]

[a] Department of Geology, University of Otago, P.O. Box 56, Dunedin, New Zealand
[b] Department of Geology, University of California – Davis, One Shields Avenue, Davis, CA 95616, USA
[c] Department of Geological Sciences, University of Florida, P.O. Box 112120, Gainesville, FL 32611-2120, USA
[d] Department of Marine Science, University of Otago, P.O. Box 56, Dunedin, New Zealand
[e] Center for Advanced Marine Core Research, Kochi University, B200 Monode, Nankoku, Kochi 783-8502, Japan
[f] Geological Survey of Japan, AIST Atmosphere and Ocean Research Institute, University of Tokyo Kashiwa 277-8564, Japan

ARTICLE INFO

*Article history:*
Received 10 August 2012
Received in revised form
23 April 2013
Accepted 24 April 2013
Editor: J. Lynch-Stieglitz
Available online 1 July 2013

*Keywords:*
Exp 320
U1336
magnetostratigraphy
RPI
middle-Miocene
GPTS

ABSTRACT

We present a high-resolution magnetostratigraphy and relative paleointensity (RPI) record derived from the upper 85 m of IODP Site U1336, an Equatorial Pacific early to middle Miocene succession recovered during Expedition 320/321. The magnetostratigraphy is well resolved with reversals typically located to within a few centimeters resulting in a well-constrained age model. The lowest normal polarity interval, from 85 to 74.87 m, is interpreted as the later part of Chron C6n (18.614–19.599 Ma). Thirty-three other magnetozones occur from 74.87 to 0.85 m, which are interpreted to represent the continuous sequence of chrons onset of Chron C5Er (18.748 Ma) to the end of Chron C5An.1n (12.014 Ma). We identify three putative previously-unrecognized subchrons within Chron C5Cn.1n, Chron 5Bn.1r, and C5ABn. Sedimentation rates vary from about 7 to 15 m/Myr with a mean of about 10 m/Myr. We observe rapid, apparent changes in the sedimentation rate at geomagnetic reversals between ~16 and 19 Ma that indicate a calibration error in geomagnetic polarity timescale (ATNTS2004). The remanence is carried mainly by non-interacting particles of fine-grained magnetite, which have FORC distributions characteristic of biogenic magnetite. Given the relative homogeneity of the remanence carriers throughout the 85-m-thick succession and the fidelity with which the remanence is recorded, we have constructed a relative paleointensity (RPI) record that provides new insights into middle Miocene geomagnetic field behavior. The RPI record indicates a gradual decline in field strength between 18.5 Ma and 14.5 Ma, and indicates no discernible link between RPI and either chron duration or polarity state.



## 1. Introduction

Integrated Ocean Drilling Program (IODP) Site U1336 (lat 5°18.735′N, long 126°17.002′W, Fig. 1) was drilled in April 2009 in a water depth of 4327 m as one site in the IODP Expedition 320/321 Pacific Equatorial Age Transect (PEAT) (Pälike et al., 2009, 2012). The aim of Expedition 320/321 was to recover a composite Cenozoic succession from the paleoequatorial Pacific sediment bulge (e.g., Lyle, 2003). Drilling at Site U1336 recovered a ~300 m thick early Oligocene to middle Miocene succession of pelagic sediments—a time when Antarctica was thought to have supported smaller, more dynamic ice sheets than today (e.g., Florindo et al., 2005), the Carbon Compensation Depth (CCD) was deep (e.g., Lyle, 2003) and the deep sea benthic oxygen isotope record indicates relatively heavy oxygen isotope values (e.g., Zachos et al., 2001a, 2001b; Pälike et al., 2006).

In this paper we present the magnetostratigraphy from Site U1336 which is a key chronological dataset underpinning the correlation of individual PEAT drill sites, separated by up to 2800 km, that target different intervals between the Eocene and Pleistocene. Shipboard paleomagnetic analyses revealed that diagenetic alteration below ~85 m at Site U1336 has completely removed remanence carriers from the sediments (Pälike et al., 2009). However, the upper ~85 m from Holes U1336A and U1336B contain a stable magnetization that spans the early to middle Miocene period (~19–13 Ma).

Studies by Lanci et al. (2004), from the nearby ODP Site 1218 (~780 km WNW of U1336, Fig. 1), resulted in a well-constrained magnetostratigraphy from post-cruise u-channel analyses. Initial

* Corresponding author at: Department of Geology, University of Otago, P.O. Box 56, Dunedin, New Zealand.
*E-mail address:* christian.ohneiser@gmail.com (C. Ohneiser).

0012-821X/$ - see front matter © 2013 Elsevier B.V. All rights reserved.
http://dx.doi.org/10.1016/j.epsl.2013.04.038

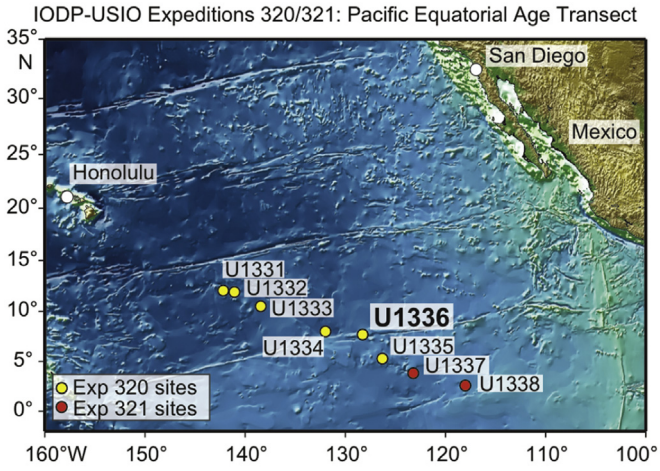


**Fig. 1.** Location map showing Site U1336, and other IODP Expedition 320/321 drill sites.

age models from Site U1336 indicated that sedimentation rates were five times greater during the early–middle Miocene at this site thereby warranting further study using continuous u-channel samples. The recovery of this pristine record, with a relatively high sedimentation rate, also provided a unique opportunity to investigate the evolution of the early to middle Miocene geomagnetic field.

The geomagnetic polarity timescale (GPTS, ATNTS2004, Lourens et al., 2004) provides a reference template and absolute ages for globally synchronous geomagnetic reversals that have become central to the construction of geologic timescales. Stratigraphic correlation within polarity zones requires interpolation or extrapolation between/from recorded reversals although in the last ~20 yr relative paleointensity (RPI) records that track the relative strength of the geomagnetic field have been used for long-distance correlation (e.g. Stoner et al., 1995). Efforts to stack globally distributed RPI records have resulted in reference records for the last 3 Myr that can be used as a dating tool (e.g. Guyodo and Valet, 1999; Yamazaki and Oda, 2005; Channell et al., 2009; Ziegler et al., 2011). RPI reference records from periods older than 3 Ma are scarce because of a paucity of successions with well-resolved RPI records, which are not biased by perturbations in sedimentation rate and/or sediment character. High quality RPI records from older periods are sorely needed so that age models can be more precisely constructed for successions throughout the Cenozoic.

## 2. Methods

Site U1336 was recovered using the Advanced Piston Corer (APC) to a depth of 184.8 m below seafloor. In all cases, when we discuss depths within drill cores, these are based on the core composite depth below seafloor (CCSF) as reported in the initial reports volume (Pälike et al., 2009). The entire succession presented here (0–85 m) was cored using a non-magnetic cutting shoe and core barrels, that minimize unwanted magnetic overprinting of the sediments. The APC, when combined with non-magnetic coring tools, is unique in its ability to sample unconsolidated sediments with minimal physical and magnetic disturbance resulting in high-quality cores with which to study the evolution of the geomagnetic field and develop magnetostratigraphies.

Site U1336 cores were demagnetized in fields of 20 mT during Expedition 320/321 as part of the initial core characterization and age model construction effort (Pälike et al., 2009). U-channel sampling of Site U1336 was conducted at the IODP Core Repository at Texas A&M University, where we collected a continuous, composite ~85 m u-channel record (from 0 to 85 m), from holes U1336A and U1336B. The u-channel samples were shipped to the Otago Paleomagnetic Research Facility (OPRF) at the University of Otago, Dunedin, New Zealand.

Magnetic moment measurements of u-channels were made at 1 cm intervals using a 2G Enterprises DC 760.5, pass-through superconducting rock magnetometer housed in a magnetically shielded room at the OPRF. U-channel were demagnetized at 5 mT increments in fields between 20 mT and 50 mT, then at 60 mT, 70 mT and finally at 100 mT using the in-line AF demagnetization coils of the 2G magnetometer. After AF demagnetization an anhysteretic remanent magnetization (ARM) was imparted using a DC bias field of 39.79 A/m (0.05 mT) in alternating fields of 100 mT with a tray speed of 8 cm/s. A tray speed of 8 cm/s (the slowest possible on the 2G magnetometer) was chosen after Brachfeld et al. (2004) demonstrated that samples do not acquire the full DC bias field to saturation with the default tray speed of 30 cm/s. A faulty calibration of the DC bias field associated with the ARM unit allowed a weak DC field to be imparted on eight u-channels during NRM demagnetization. The weak DC field resulted in negatively inclined demagnetization vectors, which did not trend to the origin of orthogonal component vector plots and therefore resulted in high MAD estimates. ARM acquisition and demagnetization was carried out after recalibration of the ARM unit, and ARMs were demagnetized in AF peak fields increasing in 10 mT steps between 20 mT and 60 mT. Magnetic susceptibility was measured on each u-channel at 2 cm intervals using a narrow aperture (24 mm diameter) Bartington susceptibility loop fitted to the Geotek multisensor core logger.

Thermomagnetic, first order reversals curves (FORCs), hysteresis and isothermal remanent magnetization (IRM) analyses were conducted on selected samples to determine the magnetic mineralogy. Thermomagnetic curves were generated at the OPRF using an AGICO MFK-1CS Kappabridge. Samples (0.25 $cm^3$) were heated to temperatures of 700 °C in air. Some samples were heated in an argon atmosphere to prevent oxidation, but this was unsuccessful probably because of clays dehydrating during heating. Hysteresis, IRM, and FORC (Pike et al., 1999; Roberts et al., 2000) measurements were made on 0.15–0.1 g crushed samples at the Istituto Nazionale di Geofisica e Vulcanologia (INGV), Rome, Italy, using a Princeton Measurements Corporation Vibrating Sample Magnetometer (VSM, MicroMag 2900). Two FORCs were measured for each sample analyzed: an initial low resolution FORC with a field spacing of 2 mT, an interaction field ($H_u$) ranging from −60 to +60 mT, and coercivity field ($H_c$) ranging from 0 to 100 mT. A second high resolution FORC, designed specifically to identify biogenic magnetite, was measured with a field spacing of 0.8 mT, $H_u$ between −15 and +15 mT, and $H_c$ between 0 and 100 mT. To define better the biogenic magnetite peak an additional higher resolution measurement was made on sample U1336B-5H-6A 80 cm with a very fine field spacing of 0.4 mT. FORC data were processed using the FORCinel software package of Harrison and Feinberg (2008). A smoothing factor (SF) of between 5 and 8 (Roberts et al., 2000) was applied to data depending on the magnetic concentration and hence noise level.

Spectral analyses of the ARM and RPI data were performed using the DOS based SPECTRUM software of Schulz and Stattegger (1997) where smoothing was done using weighted overlapped segment averaging (WOSA) with a 50% overlapping window and a Hanning taper to define spectral peaks. In all spectral analyses, we use an Oversampling Factor (OFAC) of 4, a highest frequency factor (HIFAC) 1, and a level of significance ($\lambda$) of 0.05.

Demagnetization data were plotted on orthogonal vector component plots using the PuffinPlot software package (Lurcock and Wilson, 2012). Equal area stereoplots and intensity decay curves were also used to help determine the demagnetization behavior

and polarities of each sample. Polarity determinations of the primary depositional remanent magnetizations (DRM) were obtained from principal component analyses (PCA, Kirschvink, 1980) of the 20–50 mT peak field interval comprising seven demagnetization steps where ~80% of the magnetization was lost. PCAs were anchored to the origin of orthogonal vector component plots in all cases except where a DC field was inadvertently imparted on sediments resulting in offset vectors and a free fit for PCAs (see Section 4). Our RPI record was constructed using the slope of the best fit line between NRM and the ARM demagnetization data as described by Channell et al. (2002) and implemented in the UPmag software by Xuan and Channell (2009). We also use the traditional NRM/ARM normalizer to fill gaps in our record (e.g., Tauxe, 1993). Data are available at PANGAEA—Network for Geological and Environmental Data (www.pangaea.de) http://doi.pangaea.de/10.1594/PANGAEA.810526.

## 3. Magnetic mineralogy and NRM, ARM, and MS

### 3.1. NRM, ARM and MS variations

Down core NRM, ARM and MS variations are shown in Fig. 2. Shipboard measurements revealed an average NRM of ~$1 \times 10^{-3}$ A/m where the variability reflects not only variations in the primary DRM but also variations in overprints, which the sediment acquired after deposition and during or since coring of sediments. Demagnetization of sediments at the OPRF resulted in an average remaining magnetization of ~$1.2 \times 10^{-4}$ A/m after the 20 mT demagnetization step. ARMs imparted at the OPRF resulted in magnetizations of ~$5 \times 10^{-2}$ A/m and MS measurements, which more or less mirrored ARM variations, were on average $8.5 \times 10^{-5}$ (SI). Conspicuous cycles are present in both the MS and ARM data but less apparent in the NRM data. MS variations

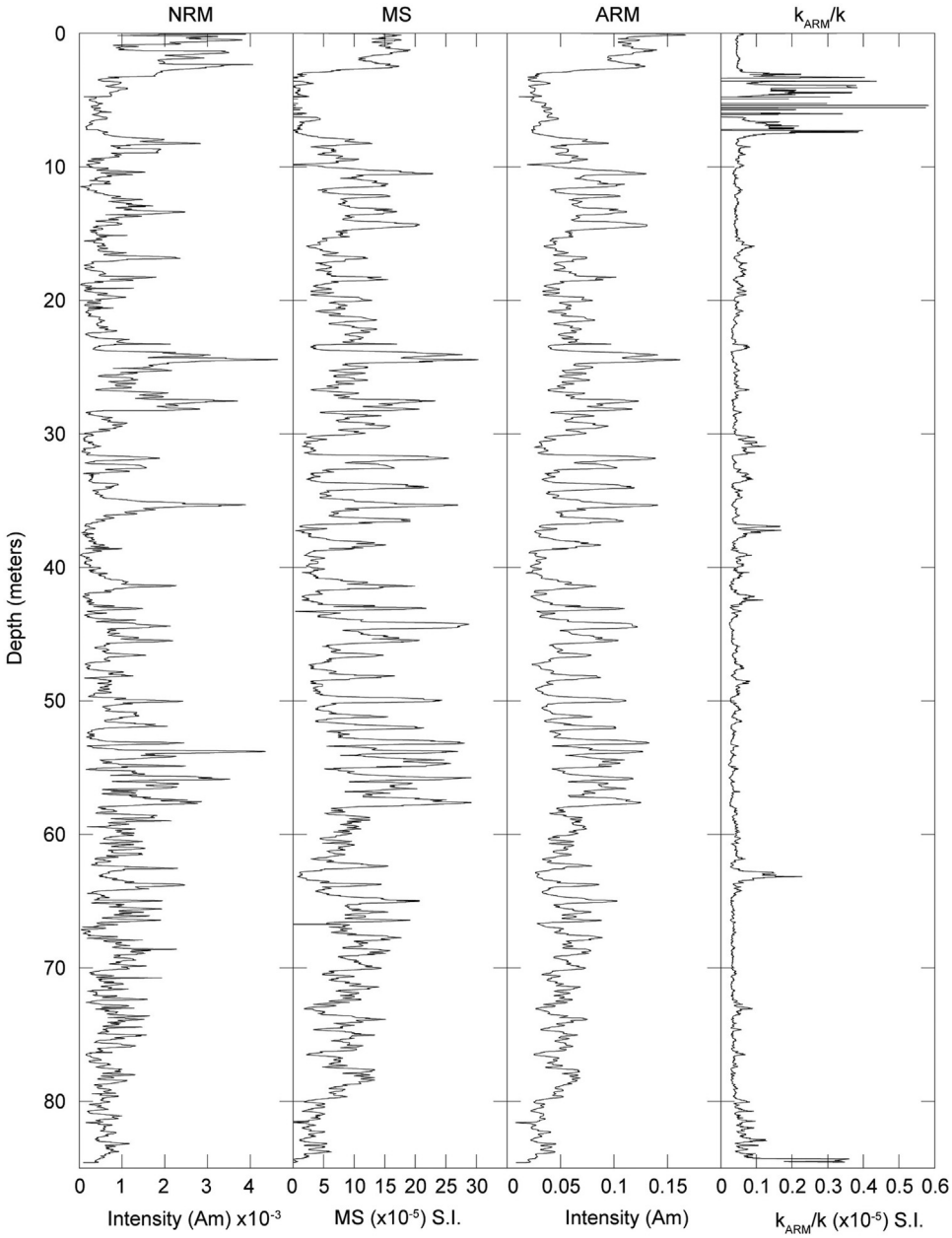


**Fig. 2.** Natural remanent magnetization (NRM) intensity (after 20 mT demagnetization), anhysteretic remanent magnetization (ARM), and volume magnetic susceptibility (MS) from Site U1336. The ARM and MS data reveal conspicuous cycles, which are paced with eccentricity (see Fig. 7). Susceptibility of ARM divided by susceptibility ($k_{ARM}/k$ is a magnetite grain-size proxy that indicates uniform down-core magnetic grain size except in the upper 7 m).

reflect changes in the concentration of magnetite in these sediments, and ARM variations largely reflect changes in the concentration of fine-grained magnetite grains when magnetite is the dominant magnetic mineral. Overall, ARM and NRM intensity does not vary by more than an order of magnitude, which is generally considered an acceptable range for accurate RPI determinations (Tauxe, 1993).

### 3.2. Magnetic mineralogy

The demagnetization behavior of Site U1336 u-channels (Fig. 3) indicates that ~80% of the original NRM is lost at peak AF fields of 60 mT, indicating that low coercivity magnetic minerals are the dominant carriers of NRM. Hysteresis and IRM analyses (Fig. 4) indicate the presence of low-coercivity magnetic minerals. The Day plot (Day et al., 1977; Dunlop, 2002a, 2002b; Fig. 4) indicates hysteresis ratios consistent with pseudo-single domain (PSD) magnetite or mixtures of PSD and single domain (SD). The magnetite grain size proxy, $k_{ARM}/k$ (Fig. 2), the ratio of the susceptibility of ARM (ARM intensity divided by the bias field) to magnetic susceptibility, indicates low values and minimal variation below ~7 m (~12.7 Ma) indicating minimal changes in magnetic grain-size down core. Above ~7 m greater $k_{ARM}/k$ variability

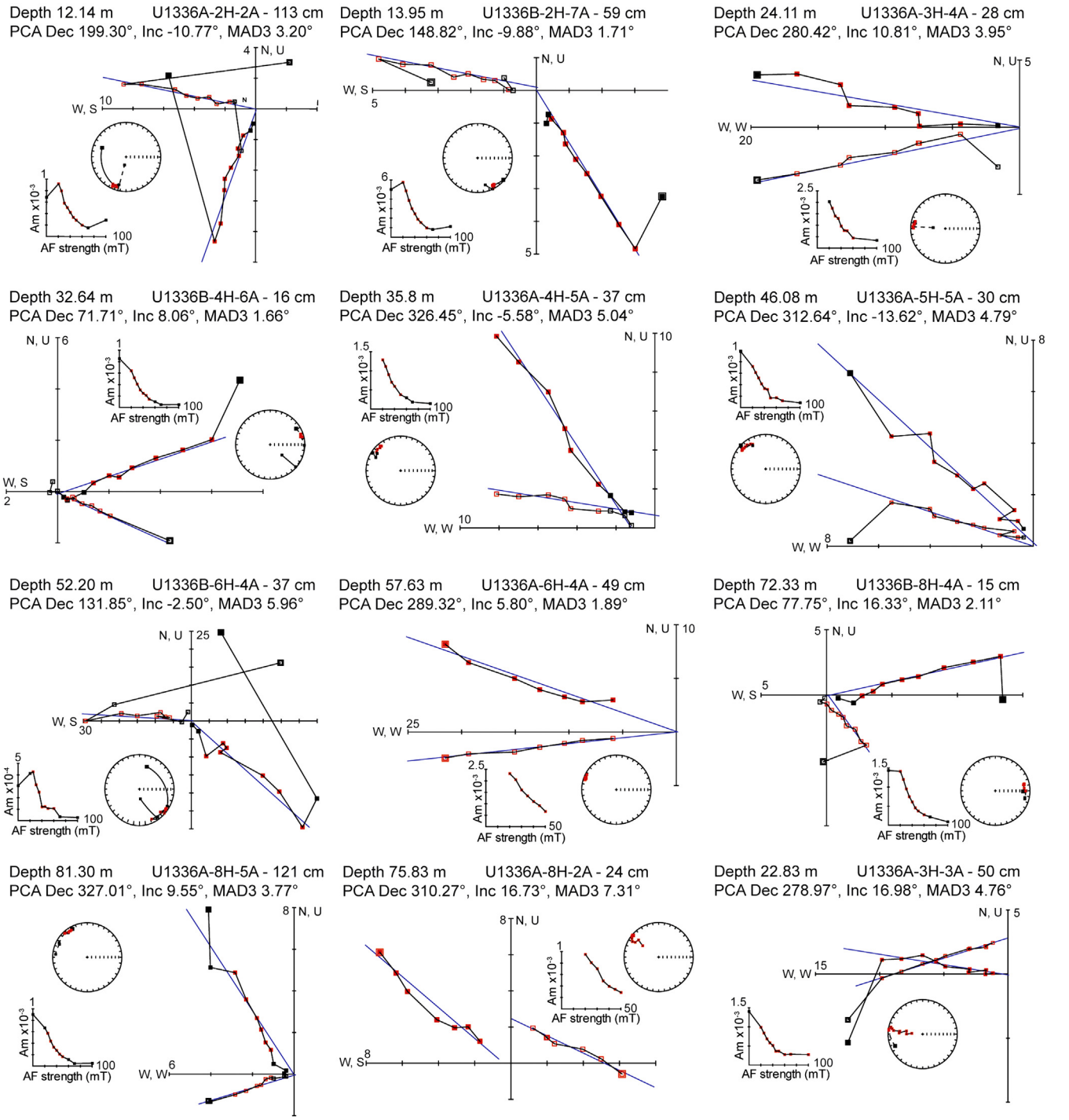


**Fig. 3.** Demagnetization behavior of Site U1336 from selected intervals. Demagnetization was effective at removing any viscous overprints by the 20 mT step and revealed a single magnetization component, albeit weakly magnetized, that was 80% demagnetized by the 60 mT peak field step. In some intervals (e.g. 75.83 m and 22.83 m) an additional high coercivity component is present that was not fully demagnetized (see text for explanation).

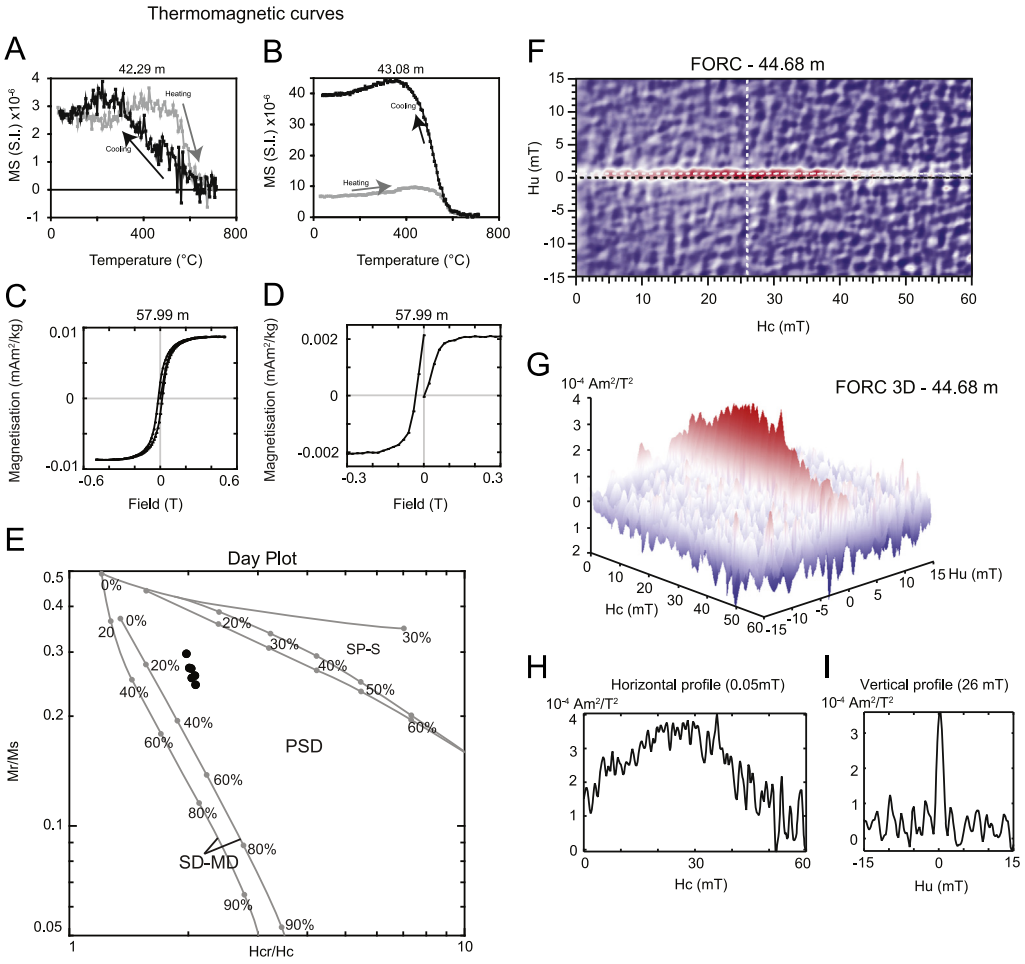


**Fig. 4.** (a) and (b) Thermomagnetic, (c) hysteresis, (d) isothermal remanent magnetization (IRM), and (f)–(i) FORC analyses of selected samples from Site U1336. (e) The Day plot (Day et al., 1977; Dunlop, 2002a, 2002b) indicates pseudo-single domain (PSD) magnetite or mixtures of PSD and single domain (SD). Thermomagnetic analyses indicate Curie temperatures of ~580 °C, which are consistent with magnetite.

(including negative values) coincide with higher density sediments, which may be caused by variable carbonate content as the drill site descended below the CCD at ~12 Ma (Pälike et al., 2009, 2012). The abrupt increase of the $k_{ARM}/k$ ratio at the base of the succession (below 85 m) coincides with the first evidence of dissolution diagenesis, which prevented a further study of older sediments. Thermomagnetic analyses (Fig. 4) indicate Curie temperatures of ~580 °C, which are consistent with magnetite and agree with IRM and hysteresis data (Fig. 4).

FORC analyses of 28 samples distributed throughout the core were used to define the magnetic mineralogy and revealed that sediments from the upper 85 m are dominated by non-interacting, single domain grains of (likely biogenic) magnetite. Furthermore, the FORC diagrams mimic those of the Lake Ely sediments, which have a magnetization carried by isolated or intact chains of magnetofossils composed of biogenic magnetite (Egli et al., 2010). Biogenic magnetite is produced by magnetotactic bacteria, which are prokaryotic organisms that live near the sediment water interface and biomineralize magnetite (and occasionally greigite under anoxic, diagenetic conditions) in a thin cellular membrane (e.g., Bazylinski et al., 1995; Bazylinski and Frankel, 2004). Biogenic magnetite is typically very pure $Fe_3O_4$ (no cation substitution) with a near perfect SD grain-size and crystal structure, the ideal magnetic grain for carrying a DRM in sediments. The very narrow central ridge of the FORC (Fig. 4i) with its uniform width along its entire length indicates that magnetostatic interactions are very weak (Egli et al., 2010). The low average Median Destructive Field (MDF) of ARM of only 26.5 mT along the entire studied section indicates the dominance of moderately soft magnetite; furthermore, the interaction (or bias) width for the main FORC distribution at half its peak value is proportional to the measurement increment as noted for the Lake Ely sediments (Egli et al., 2010). Such behavior could, of course, be representative of isolated SD and small PSD magnetite grains of any origin, including possibly eolian material. The similarity of the FORCs to the FORCs associated with biogenic magnetite implies that the primary remanence carrier is biogenic magnetite, as concluded by Channell et al. (2013) at nearby IODP Sites U1334 and U1335.

## 4. Magnetostratigraphy and paleomagnetic age model

Fig. 5 shows the component declination from Holes U1336A and U1336B, the resulting stacked declination and inclination for Site U1336, virtual geomagnetic poles (VGPs), and median angular deviation (MAD) associated with the component calculation. Paleomagnetic inclination is close to zero as expected because the site is located close to the paleoequator where the time averaged geomagnetic field is essentially horizontal and not useful for assigning polarity zones. Declination was, therefore, the only means by which to construct the magnetostratigraphy. Unfortunately, the cores were not azimuthally oriented because of problems with the orienting tool. We therefore developed a magnetostratigraphy for Site U1336 by mapping paleomagnetic reversals for each core, paying particular attention to the

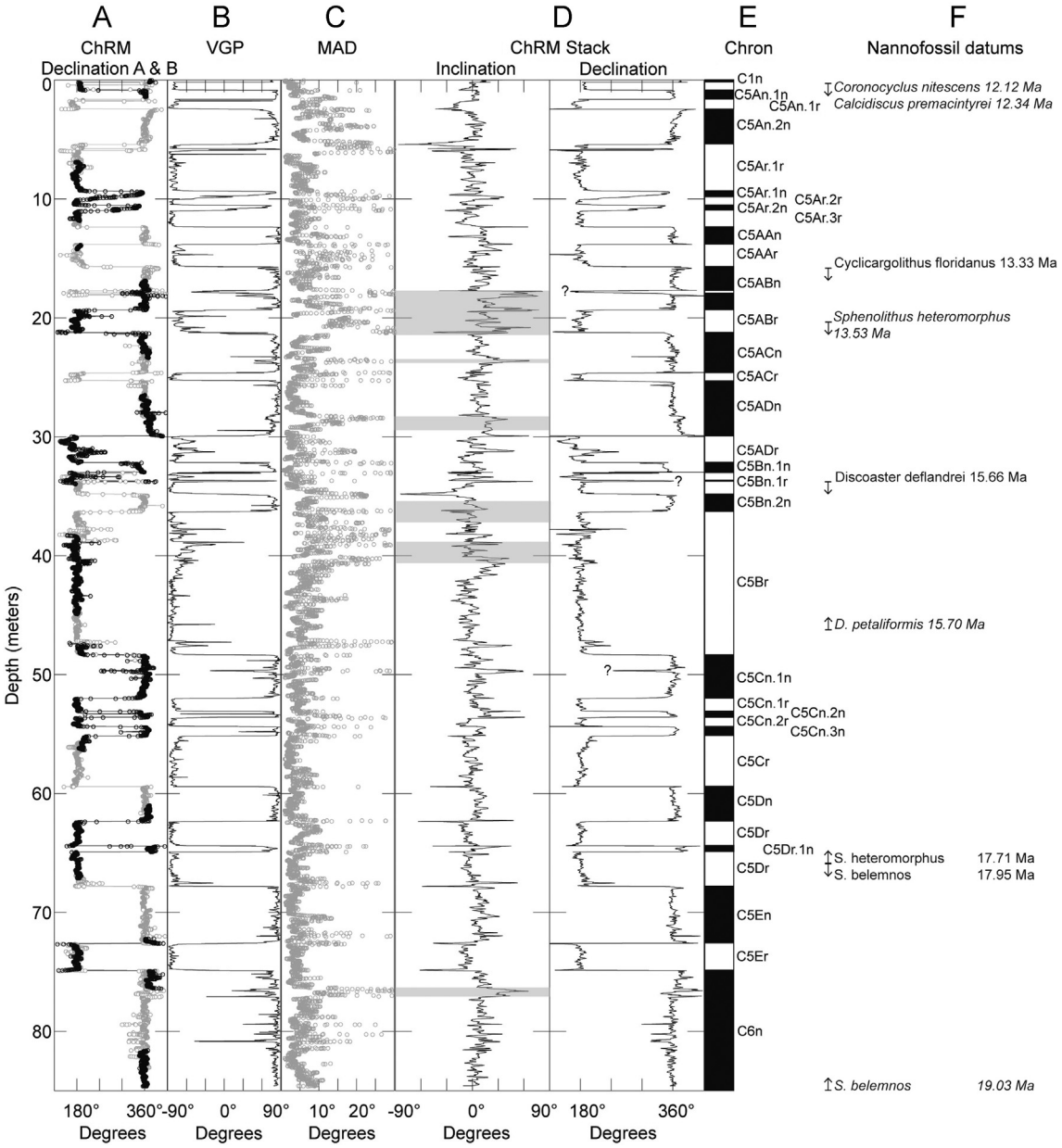


**Fig. 5.** (a) Reoriented declination from Holes U1336A (gray) and U1336B (black), (b) virtual geomagnetic dipole (VGP) calculated from the reoriented declination stack, (c) MAD estimates from PCA calculations, (d) stacked inclination and declination, and correlation with the GPTS (e) where black intervals indicate normal polarity and white intervals indicate reversed polarity. (f) Key nannofossil FADs and LADs are also shown which help constrain the correlation. At the base of the U1336, faint shallow, negative and positive inclination alternations (e.g. the C5En–C5Er–C6n reversals pattern) help confirm the correlation with the GPTS. Subchrons not found in the standard GPTS are indicated by "?". Shaded intervals indicate where a weak ARM was unintentionally imparted on the sediments during demagnetization (see text for discussion).

overlapping segments between cores from Holes U1336A and B. By coring and stratigraphically correlating multiple holes, then splicing the recovered material into one composite stratigraphic section, as was done during Expedition 320 (Pälike et al., 2009), a continuous record of declination could subsequently be obtained. One needs only to correlate the resulting ~180° alternation in declination to the geomagnetic polarity timescale (GPTS), which can be facilitated with biostratigraphic information. Our correlation with the geomagnetic polarity time scale (GPTS, ATNTS2004, Lourens et al., 2004), was guided by first and last appearance datums (FAD and LAD, respectively) of microfossils in core catcher samples as reported in the initial reports volume (Pälike et al., 2009). By utilizing the overlap of cores between Holes U1336A and U1336B, a composite declination stack was constructed where only one, unique polarity pattern was possible, which could, in turn, be confidently correlated with the GPTS. Individual cores were then reoriented back into approximate geographic coordinates more accurately by subtracting the mean declination from each observed declination resulting in normal polarity intervals with ~0° declination and reversed polarity intervals with ~180° declination. This is only an approximate return to geographic coordinates because the Pacific Plate has moved relative to the spin axis over the past 20 Myr but only by an amount that would cause the mean declination to deviate from 0° by at most about 15° (Acton and Gordon, 1994; Horner-Johnson and Gordon, 2010).

Low MAD values typically less than 10° (Fig. 5) indicate the high quality of the demagnetization data. Discrete intervals with high (above 15°) MAD values (Fig. 5) occur at geomagnetic reversals and in thin intervals with poor demagnetization behavior or are attributed to a faulty calibration of the ARM unit where

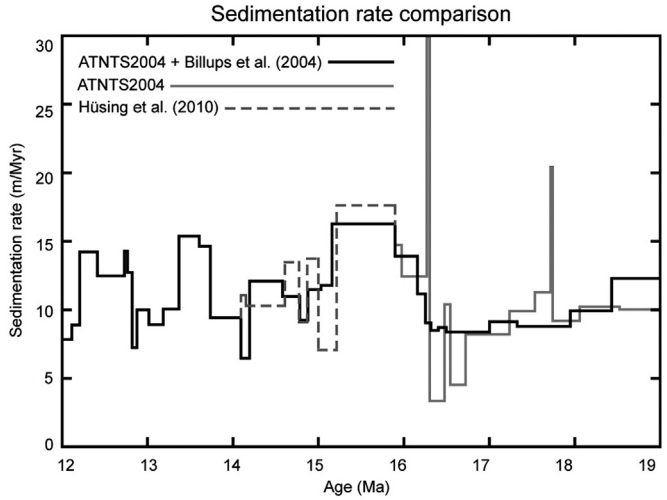


**Fig. 6.** Our preferred age model for Site U1336 uses ATNTS2004 (Lourens et al., 2004) down to the top of Chron C5Br and the astronomical calibration of Billups et al. (2004) prior to the base of C5Br (black line). The ATNTS2004 calibration of Lourens et al. (2004) from the base of C5Br is shown with a gray line to illustrate the abrupt changes in sedimentation rate. The astronomical calibration proposed by Billups et al. (2004) produces far smoother sedimentation rates and is probably more correct. The dashed line illustrates the sedimentation rates for the alternative calibration of C5Bn.2n through C5ADn as proposed by Hüsing et al. (2010).

a very weak DC field was imparted on eight u-channels (see Section 2). Fig. 5 shows the correlation of the Site U1336 declination stack with the polarity timescale (Lourens et al., 2004). Inclination data are also shown because at the base of the drill core the faint shallow negative–positive–negative inclination (e.g. the C6n–C5Er–C5En reversals pattern) helps confirm the correlation with the GPTS.

In the upper 20 m of Site U1336, our correlation is constrained by the LADs of *Coronocyclus nitescens* and *Calcidiscus premacintyrei* at 1.10 m depth, which have ages of 12.12 Ma and 12.45 Ma, respectively, according to Lourens et al. (2004). Based on these ages, we interpret the normal polarity interval from 0.85 to 1.65 m to be Chron C5An.1n (12.014–12.116 Ma). Somewhere above this normal polarity interval or perhaps even within it a hiatus of ~10 Myr in duration occurs but the exact age and duration cannot be constrained by either biostratigraphy or magnetostratigraphy. The LADs of *Cyclicargolithus floridanus* (13.33 Ma) and *Sphenolithus heteromorphus* (13.53 Ma), which occur at 16.30 m and 20.62 m, respectively, allow for a confident correlation of the reversal pattern with polarity chrons C5Ar.3r through C5ABn. The thick normal polarity zone with the thin intervening reversed polarity zone between 21.30 m and 30.00 m is correlated with chrons C5ACn–C5ACr–C5ADn. Chron C5ACr was not identified during shipboard analyses but was resolved by the u-channel measurements in the interval from 25.27 to 24.63 m. The FAD of *Discoaster petaliformis* at ~46.2 m indicates an age of 15.7 Ma. We therefore correlate the thick reversed polarity interval (at 36.3–48.3 m) with Chron C5Br and the overlying reversals pattern with Chrons C5Bn.2n through C5ADr. Below Chron C5Br, our correlation with the GPTS is relatively unambiguous and is helped by the very shallow positive and negative inclination changes at some reversals. The FADs of *S. heteromorphus* and LAD of *Sphenolithus belemnos* at 66.56 m have ages of 17.71 Ma and 17.95 Ma, respectively (Lourens et al., 2004), and indicate that the thick reversed polarity zone and the thin normal polarity subzone between 62.3 m and 67.8 m correlate with Chron C5Dr and Subchron C5Dr.1n, respectively. The FAD of *Sphenolithus disbelemnos* at the base of the studied interval has an age of 19.03 Ma. We therefore correlate the thick normal polarity interval (below 74.87 m) with Chron C6n. The base of Chron C6n was not identified because sediments are too weakly magnetized to allow determination of NRM below 85 m. A table of the depths of correlated geomagnetic reversals is presented in the Supplementary material (Table S1).

We identify three new subchrons of the geomagnetic field (Fig. 5) in our magnetostratigraphy and have assigned ages to these based on linear interpolation between the adjacent geomagnetic reversals. A thin reversed polarity interval is identified at 17.8 m within Chron C5ABn and has an age of 13.50 Ma. A thin normal polarity interval is recognized at 33.72 m in Chron C5Bn.1r to which we assign an age of 14.94 Ma and a thin interval with intermediate polarity is identified at 49.67 m within Chron C5Cn.1n to which we assign an age of 15.99 Ma. The normal polarity interval with C5Bn.1r is also observed at Site U1335 (Channell et al., 2013).

Magnetization lock-in postdates deposition by a time corresponding to the thickness of the bioturbated surface sediment layer, which is usually about 10 cm thick and independent of sedimentation rate (see discussion in Channell and Guyodo, 2004). In these sediments, 10 cm may be expected to correspond to ~10 kyr.

### 4.1. Verification of the GPTS calibration

Our correlation with the GPTS implies abrupt changes in sedimentation rates at early Miocene reversals (e.g. C5Cn.1n–C5Cn.1r–C5Cn.2n–C5Cn.2r–C5Cn.3n; Fig. 6) leading to questions about either the validity of the magnetostratigraphy or the calibration of the ATNTS2004 GPTS (Lourens et al., 2004). A careful assessment of the magnetostratigraphy and lithology with particular focus on demagnetization behavior close to magnetic reversals revealed nothing to lead us to question the validity of the Site U1336 polarity record (Supplementary Fig. S1). Therefore, we investigated the uncertainties associated with the ATNTS2004 (Lourens et al., 2004) calibration. The Miocene interval of ATNTS2004 was constructed from interpolated ages that were derived from the Australia Antarctic plate seafloor and are not astronomically calibrated.

Billups et al. (2004) suggested an alternative calibration of polarity chrons in this interval from their work from the Antarctic ODP Site 1090 succession, where they developed an astronomical calibration for the middle Miocene to Oligocene GPTS. Likewise Hüsing et al. (2010) suggested that ATNTS2004 (Lourens et al., 2004) was in error between Chrons C5Bn.2n and C5ADn from their study of the La Vedova section in northern Italy. They developed a magneto-bio-cyclostratigraphy of the succession, which they tuned to various orbital frequencies and used to recalibrate Chrons C5Bn.2n, C5Bn.1r, C5Bn.1n, C5ADr, and C5ADn.

Because sediments at Site U1336 are purely pelagic comprising exclusively nannofossil and diatom ooze (Pälike et al., 2009) and because Site U1336 is so far from the large continental land masses, the long-term average sediment input and sedimentation rate should vary smoothly without unconformities and/or changes in sediment type allowing us to test the various revisions in GPTS calibration (Lourens et al., 2004; Billups et al., 2004; Hüsing et al., 2010). The calibration of Billups et al. (2004) from the base of Chron C5Br to the top of Chron C6n produced far more consistent sedimentation rates (Fig. 6). We have therefore adopted this calibration from the base of Chron C5Br downwards. The calibration of Hüsing et al. (2010) from Chrons C5Bn.2n through C5ADn produces abrupt changes in sedimentation rate at reversal boundaries indicating that it is probably less accurate than ATNTS2004 (Lourens et al., 2004). The resulting age model applied to the Site U1336 magnetostratigraphy is based on the ATNTS2004 (Lourens et al., 2004) calibration to the top of Chron C5Br and on the calibration of Billups et al. (2004) from the base of Chron C5Br

down-section. A similar conclusion regarding issues with the ATNTS2004 timescale in this interval has been drawn by Channell et al. (2013) based on the magnetic stratigraphy at sites U1334 and U1335. As synchronous sedimentation rate changes are unlikely to have occurred at three sites in the Equatorial Pacific (Sites U1334, U1335, and U1336) and in the South Atlantic (ODP Site 1090), it is very likely that ATNTS2004 needs adjustment.

Chron C5Dr.1n is recognized in the U1336 magnetostratigraphy as well as at Sites U1334 and U1335 (Channell et al., 2013), which allows us to improve the calibration for this short polarity interval. Lourens et al. (2004) assigned an age of 17.400 Ma for both the upper and lower ages, and Channell et al. (2003) assigned 17.501 Ma and 17.556 Ma as the upper and lower ages, respectively, from studies of ODP Site 1090. At Site U1336, C5Dr.1n is better defined than at ODP Site 1090 allowing us to improve the calibration by linear interpolation between the top and bottom of chron C5Dr. Our resulting preferred upper and lower ages for C5Dr.1n are 17.560 Ma and 17.617 Ma, respectively, implying a duration of 57 kyr.

## 5. Relative paleointensity (RPI) record

The NRM intensity of a sedimentary DRM depends on the concentration, type and grain-size of magnetic minerals, and on the strength of the Earth's magnetic field. If the NRM is carried by SD or PSD magnetite and can be normalized for changes in concentration of remanence carrying grains, the relative intensity of the magnetizing field (RPI) can be determined (King et al., 1983; Tauxe, 1993; Channell et al., 2008). Previous studies have shown that by stacking multiple RPI records (e.g. the SINT-2000 stack of Valet et al. (2005), PISO-1500 of Channell et al. (2009), and PADM2M of Ziegler et al. (2011)) common, global features (either peaks or troughs) can be identified providing an additional tool for stratigraphic correlation, and dating, of sedimentary successions between geomagnetic reversals. Before RPI can be estimated, the environmentally driven changes in the magnetization (e.g. variations in the concentration of remanence-carrying grains through time) must be removed. This is accomplished by normalizing the NRM with a laboratory-induced magnetization (ARM or IRM). By normalizing the NRM through the laboratory-induced magnetization (in this study we have used ARM), the RPI can be estimated because all environmentally driven changes in concentration and grain-size are removed from the record. As described above, the upper 85 m of Site U1336 are characterized by non-interacting (possibly biogenic) SD to small PSD magnetite making Site U1336 the ideal site from which to construct an RPI record for the middle Miocene.

To ensure that our normalization procedure has removed any orbitally paced magnetic concentration cycles, we conducted spectral analysis of ARM and RPI data between 15 and 16 Ma, an interval with strong cycles. Fig. 7 shows the spectral power of ARM which indicates eccentricity paced cycles that are five orders of magnitude above a white noise background. The spectral power of RPI does not indicate statistically significant orbital peaks, for the same interval, implying that the RPI record reflects changes in magnetization of sediments driven by variations of the geomagnetic field. The Site U1336 RPI record is the most robust and of the highest quality yet published for this period, and therefore we can use it to assess the behavior of the middle Miocene geomagnetic field.

Fig. 8 illustrates the RPI stack for Site U1336 with RPI estimates made using the traditional NRM normalized by ARM (e.g., Tauxe, 1993) and the slope fit method of Channell et al. (2002) as implemented in the UPmag software by Xuan and Channell (2009). The slope of best fit is based on NRM and ARM demagnetization steps at 20, 30, 40, 50, and 60 mT. The correlation coefficient ($r$) is shown to indicate the robustness of best-fit line

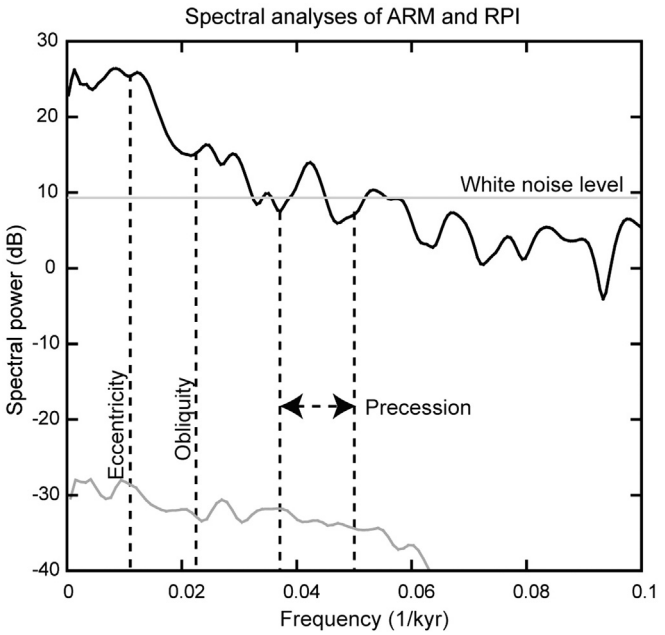


**Fig. 7.** Spectral power of anhysteretic remanent magnetization (ARM) and relative paleointensity (RPI) data from 15 Ma to 16 Ma. Spectral analysis of ARM data illustrates the strong eccentricity cycles are well above the white noise level and analysis of RPI data for the same interval indicates that the any cyclic components are below the white noise level, and not statistically significant.

and the polarity reversals record is from Fig. 5. Average sedimentation rates at Site U1336 are around ~10 m/Myr (~1 cm/kyr) allowing us to resolve the RPI of the geomagnetic field on timescales of ~5–6 kyr when taking into account the Gaussian-shaped response functions of pickup coils (at half-peak width) in the OPRF 2G magnetometer ($X$=4.628, $Y$=−4.404, and $Z$=-6.280 cm).

RPI estimates are more reliable after ~13.7 Ma (above the base of Chron C5ABr) and from the base of Chron C5Br to the base of the studied interval ($r$-values of $>0.95$). A gap in our slope RPI estimates in Chron C5Br (between 15.50 Ma and 15.65 Ma) was caused by inadvertently sampling this interval for other analyses before the second phase of ARM acquisition and demagnetization (see Section 2).

Fig. 8 further illustrates that low intensity intervals coincide with geomagnetic reversals as expected. The decline and recovery from geomagnetic reversals is variable, however, in the older, more reliable portion of the record, where reversals are generally characterized by a rapid decline in field strength followed by a slower recovery. The three subchrons or excursions identified earlier are also all associated with some of the weakest parts of the RPI record indicating a collapse of the geomagnetic field. Visually, the record also indicates that each polarity interval has a rather unique character with some chrons having higher variability and a greater average intensity than others. We see no evidence of 'saw tooth' patterns or decaying field strength leading up to geomagnetic reversals in our record as was inferred by Valet and Meynadier (1993). However, we are unable to exclude definitively the existence of sawtooth or cyclic decay–recovery patterns from our data because additional, independent age control is unavailable in our study.

To determine further whether individual polarity chrons have a unique or repeating RPI character, we conducted simple statistical tests of the RPI slope data for polarity intervals (Fig. 9) with the interval the base of Chron C5ADn (14.581 Ma) to the base of Chron C5Er (18.614 Ma) containing the most robust RPI data. C6n is excluded because the basal reversal was not identified. Statistics were calculated for each polarity interval by dividing the record by the value at the reversal boundary where RPI is at its lowest.

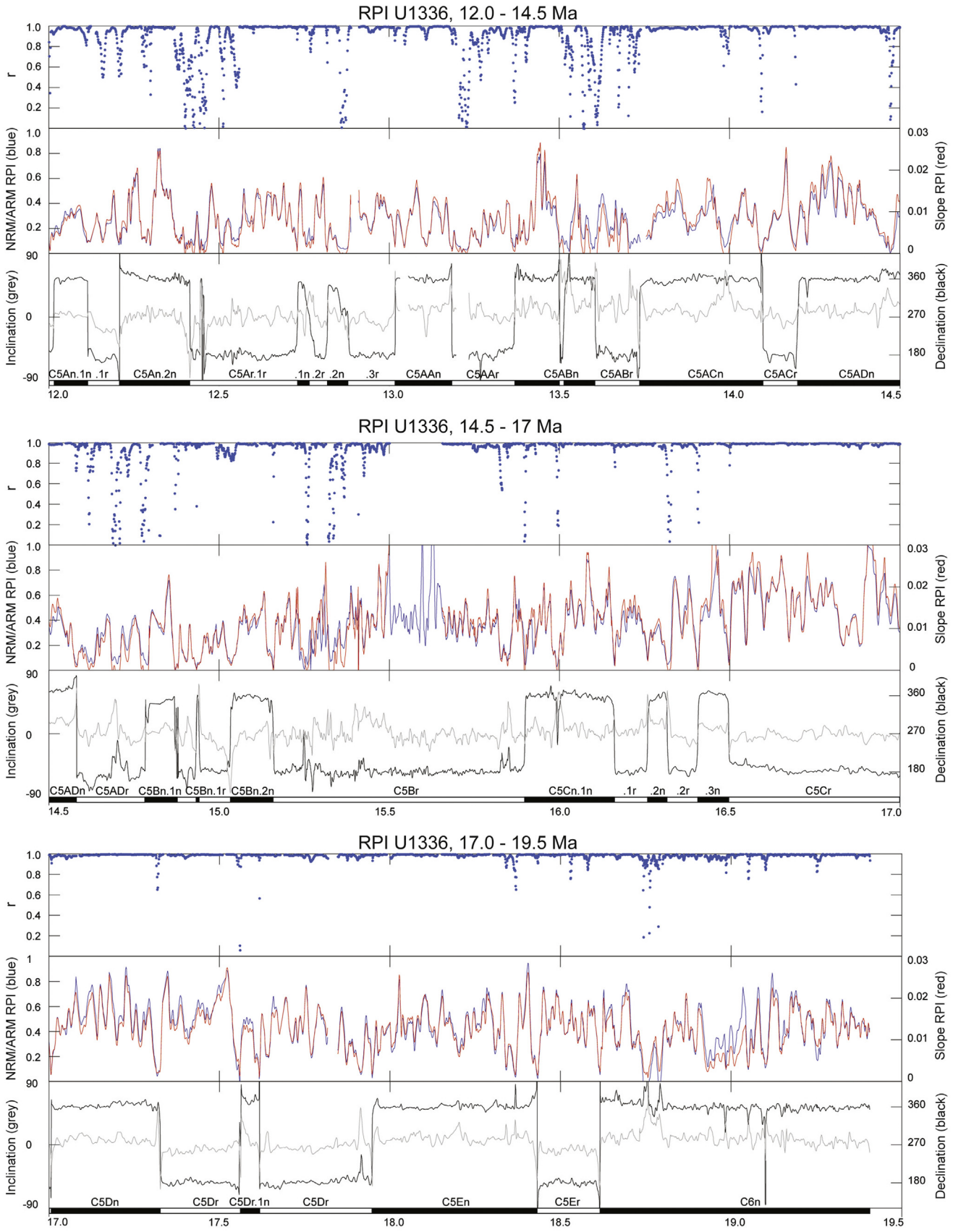


**Fig. 8.** Relative paleointensity (RPI) record from Site U1336 divided into 2.5 Myr intervals. Declination (black) and inclination (gray) and the correlation with the GPTS are shown in each interval. Both the slope (red—determined from the 20, 30, 40, 50, and 60 mT steps) and NRM/ARM (blue—20 mT step) RPI records are shown and the linear correlation coefficient (*r*-value), which indicates the robustness of the slope fit. Conspicuous and abrupt collapses of the geomagnetic field are associated with each geomagnetic reversal. (For interpretation of the references to color in this figure legend, the reader is referred to the web version of this article.)

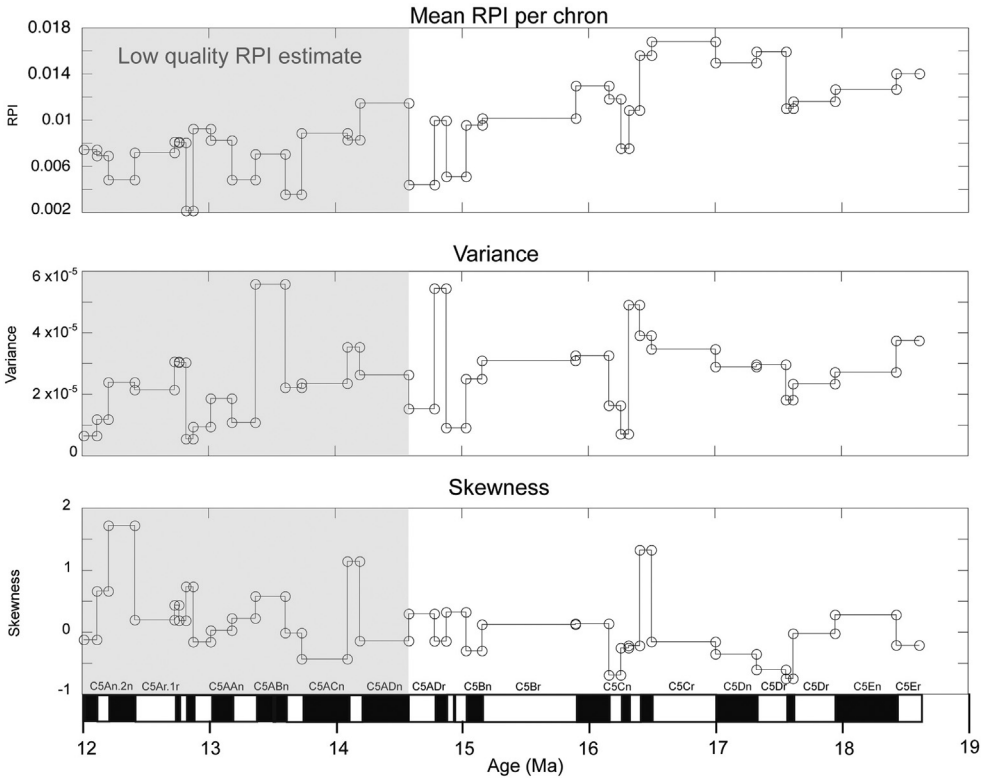


**Fig. 9.** Mean, variance, and skewness of relative paleointensity (RPI) data for each chron from the top of Chron C5An.1n (12.014 Ma) to the base of Chron C5Er (18.614 Ma). The gray area indicates the interval with less robust (poor) RPI estimates. The data show higher RPIs in older chrons with a gradual upcore reduction. Variance and skewness of each chron show no clear correlation with the duration of a chron or polarity state. The data also show that the younger and older segments of Chron C5Dr have different behavior with a mean RPI of 0.011 and 0.016 (older to younger respectively); Chron C5Dr.1n is the apparent divider.

The analyses reveal that mean RPI values generally decline as chrons become younger over this 14–19 Ma interval. This result conflicts with Tauxe (2006) who compiled absolute paleointensity estimates from DSDP/ODP submarine basaltic samples and found an increase in field strength between ~20 Ma and ~15 Ma. Additional RPI records covering this interval are needed to exclude subtle, long-term changes in magnetic mineralogy at Site U1336 as a cause of declining apparent geomagnetic field strength. We see no relationship between duration of a chron and the mean RPI (Supplementary Fig. S3), in contrast with the conclusions of Tauxe and Hartl (1997) and Constable et al. (1998). Nor do we see any relationship between the duration of a polarity chron and the variance about the mean or the skewness of the RPI data (Fig. 9).

Ziegler et al. (2011) suggested from 86 stacked relative paleointensity records, spanning the last 2 Myr, that the Brunhes Chron had ~20% stronger geomagnetic intensity than the Matuyama Chron. Likewise the SINT-2000 (Valet et al., 2005) also indicated a weaker field strength during the Matuyama Chron when compared with the Brunhes Chron. On the other hand, the PISO-1500 paleointensity stack (Channell et al., 2009) does not indicate a difference of mean intensity for Brunhes and Matuyama chrons over the last 1.5 Myr. To test further the distribution and relationship of RPI estimates and polarity we have plotted the slope determined RPI distribution from all data and for a selected interval with high quality RPI estimates between the top of Chron C5Cn.1n (15.898 Myr) to the base of Chron C5Er (18.614 Ma) (Fig. 10). We selected the Chron C5Cn.1n to Chron C5Er interval because there are an approximately equal number of reversed and normal polarity samples with roughly equal data density (1202 normal polarity and 1229 reversed polarity RPI estimates) and because this interval has the lowest overall *r*-value and therefore contains the most robust RPI estimates. Our distribution is based on 30 equally spaced bins (0.03/bin) of the slope fit data. Fig. 10 illustrates that the difference between polarities is relatively small although on average reversed polarity intervals have stronger RPI than normal polarity intervals and that the reversed polarity data are skewed in favor of higher intensities. This may, of course, only be a feature of the specific interval we have analyzed.

## 6. Conclusions

The Site U1336 magnetostratigraphy presented here provides precise depth control of geomagnetic reversals recorded in the upper 85 m that spans the ~12–19.4 Ma interval. The magnetization of the sediment is carried almost exclusively by SD and small PSD magnetite, probably of biogenic origin. Our magnetostratigraphy is correlated with the GPTS with a precision of a few centimeters and contains three subchrons that do not feature in contemporary timescales, to which we assign linearly interpolated ages of 13.50 Ma, 14.94 Ma, and 15.99 Ma. We have tested the calibration of the ATNTS2004 GPTS (Lourens et al., 2004) by observing changes in sedimentation rate at reversal boundaries. We find that the astronomical calibration proposed by Billups et al. (2004) produces much smoother changes in sedimentation between polarity reversals, and is therefore probably more correct (see also Channell et al., 2013). On the other hand, the astronomical calibration suggested by Hüsing et al. (2010) between C5Bn.2n and C5ADn produces abrupt changes in sedimentation rate at reversals, which may indicate that it is not reliable. The magnetostratigraphic age model indicates that sedimentation rates were between 7 m/Myr and 16 m/Myr and were on average ~10 m/Myr before the site descended beneath the CCD at ~12 Ma.

The apparent dominance of SD (biogenic) to small PSD magnetite as the remanence carrier allowed us to construct a well-constrained RPI record of the succession. Our data indicate that

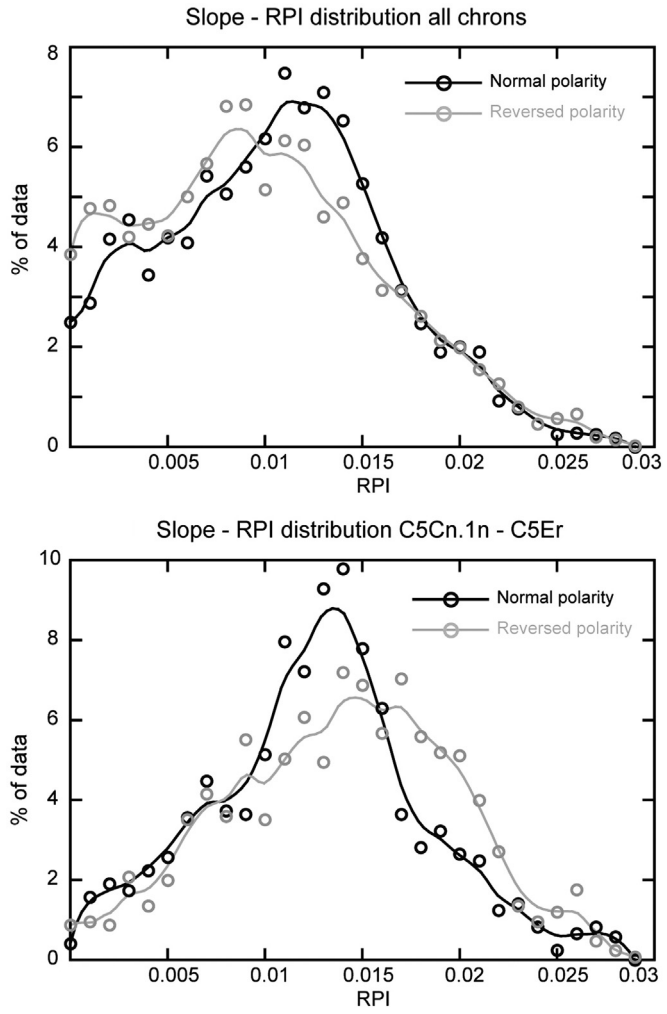


**Fig. 10.** RPI distribution for normal (black) and reversed (gray) polarity RPI estimates for the entire data set and for the most robust RPI data between the top of Chron C5Cn.1n and the base of Chron C5Er. Data plotted for the entire interval are likely contaminated by poor RPI estimates and may be biased because more RPI estimates are derived from normal polarity chrons, than reversed polarity chrons. We focus our analysis between Chrons C5Cn.1n to the base of Chron C5Er because this interval has the highest quality RPI estimates and because data are split roughly 50/50 between normal and reversed polarity states, with similar proportions for each polarity state.

the geomagnetic field may have declined in strength between 18.5 and 14.5 Ma. We see no relationship between the strength of the geomagnetic field and the duration of the chron or the polarity state, and suggest that, when viewed over a long periods, each polarity chron has a unique RPI character.

The Site U1336 RPI record is a first step in developing a global-average stacked paleointensity record for the early–middle Miocene. When enough records with a wide geographic distribution become available a stacking procedure such as those employed to produce the SINT-2000 (Valet et al., 2005), PISO-1500 (Channell et al., 2009) and PADM2M (Ziegler et al., 2011) records may result in a valuable additional dating tool for early and middle Miocene successions.

## Acknowledgments

This research used samples and data provided by the Integrated Ocean Drilling Program (IODP). Funding for this work was provided by grants from the University of Otago and from the U.S. NSF (OCE 0961161, OCE 0961412, OCE 0960999) and by U.S. Science Support Program (USSSP) Post Expedition Activity (PEA) awards. Participation of T.Y and Y.Y. to IODP Exp. 320/321 was supported by J-DESC and CDEX/JAMSTEC. We thank Fabio Florindo for helpful comments and revisions to this manuscript and Leonardo Sagnotti for technical support with FORC analyses. We thank the IODP technicians and staff and the Expedition 320/321 Shipboard Scientific Party, who provided a plethora of information through shipboard analyses and discussions. We also thank the *JOIDES Resolution* crew for their efforts in collecting the core upon which this study is based. We gratefully acknowledge the constructive criticism provided by the anonymous reviewers who helped improve this manuscript.

## Appendix A. Supplementary materials

Supplementary data associated with this article can be found in the online version at http://dx.doi.org/10.1016/j.epsl.2013.04.038.

## References

Acton, G.D., Gordon, R.G., 1994. Paleomagnetic tests of Pacific Plate reconstructions and implications for motion between hotspots. Science 263, 1246–1254.
Bazylinski, D., Frankel, R., 2004. Magnetosome formation in prokaryotes. Nat. Rev. Microbiol. 2, 217–230.
Bazylinski, D., Frankel, R., Heywood, B., Mann, S., King, J., Donaghay, P., Hanson, A., 1995. Controlled biomineralization of magnetite ($Fe_3O_4$) and gregite ($Fe_3S_4$) in a magnetotactic bacterium. Appl. Environ. Microbiol. 61, 3232–3239.
Billups, K., Pälike, H., Channell, J.E.T., Zachos, J.C., Shackleton, N.J., 2004. Astronomic calibration of the late Oligocene through early Miocene geomagnetic polarity time scale. Earth Planet. Sci. Lett. 224, 33–44.
Brachfeld, S.A., Kissel, C., Laj, C., Mazaud, A., 2004. Behavior of u-channels during acquisition and demagnetization of remanence: implications for paleomagnetic and rock magnetic measurements. Phys. Earth Planet. Inter. 145, 1–8.
Channell, J.E.T., Galeotti, S., Martin, E.E., Billups, K., Scher, H.D., Stoner, J.S., 2003. Eocene to Miocene magnetostratigraphy, biostratigraphy, and chemostratigraphy at ODP Site 1090 (sub-Antarctic South Atlantic). Geol. Soc. Am. Bull. 115, 607–623.
Channell, J.E.T., Guyodo, Y., 2004. The Matuyama chronozone at ODP Site 982 (Rockall Bank): evidence for decimeter-scale magnetization lock-in depths. In: Channell, J.E.T., Kent, D.V., Lowrie, W., Meert, J. (Eds.), Timescales of the Paleomagnetic Field, vol. 145. AGU Geophysical Monograph Series, pp. 205–219.
Channell, J.E.T., Hodell, D., Xuan, C., Mazaud, A., Stoner, J.S., 2008. Age calibrated relative paleointensity for the last 1.5 Myr at IODP Site U1308 (North Atlantic). Earth Planet. Sci. Lett. 274, 59–71.
Channell, J.E.T., Mazaud, A., Sullivan, P., Turner, S., Raymo, M.E., 2002. Geomagnetic excursions and paleointensities in the Matuyama Chron at Ocean Drilling Program Sites 983 and 984 (Iceland Basin). J. Geophys. Res. 107, 2114, http://dx.doi.org/10.1029/2001JB000491.
Channell, J.E.T., Xuan, C., Hodell, D.A., 2009. Stacking paleointensity and oxygen isotope data for the last 1.5 Myr (PISO-1500). Earth Planet. Sci. Lett. 283, 14–23.
Constable, C.G., Tauxe, L., Parker, R.L., 1998. Analysis of 11 Myr of geomagnetic intensity variation. J. Geophys. Res. 103, 171735–171748.
Channell, J.E.T., Ohneiser, C., Yamamoto, Y., Kesler, M.S., 2012. Oligocene–Miocene magnetic stratigraphy carried by biogenic magnetite at Sites U1334 and U1335 (equatorial Pacific Ocean). Geochem. Geophys. Geosyst. 14 (2), http://dx.doi.org/10.1029/2012GC004429.
Day, R., Fuller, M., Schmidt, V.A., 1977. Hysteresis properties of titanomagnetites: grain-size and compositional dependence. Phys. Earth Planet. Inter. 13, 260–267.
Dunlop, D.J., 2002a. Theory and application of the Day plot ($M_{rs}/M_s$ versus $H_{cr}/H_c$) 1. Theoretical curves and test using titanomagnetite data. J. Geophys. Res 107, 2056, http://dx.doi.org/10.1029/2001JB000486.
Dunlop, D.J., 2002b. Theory and application of the Day plot ($M_{rs}/M_s$ versus $H_{cr}/H_c$) 2. Application to data for rocks, sediments, and soils. J. Geophys. Res 107, 2057, http://dx.doi.org/10.1029/2001JB000487.
Egli, R., Chen, A., Winklhofer, M., Kodama, K.P., Horng, C.S., 2010. Detection of noninteracting single domain particles using first-order reversal curve diagrams. Geochem. Geophys. Geosyst. 11, 1–22.
Florindo, F., Wilson, G.S., Roberts, A.P., Sagnotti, L., Verosub, K.L., 2005. Magnetostratigraphic chronology of a late Eocene to early Miocene glacimarine succession from the Victoria Land Basin, Ross Sea, Antarctica. Global Planet. Change 45, 207–236.
Guyodo, Y., Valet, J.P., 1999. Global changes in intensity of the Earth's magnetic field during the past 800 kyr. Nature 399, 249–252.
Harrison, R., Feinberg, J., 2008. FORCinel: an improved algorithm for calculating first-order reversal curve distributions using locally weighted regression smoothing. Geochem. Geophys. Geosyst. 9, 1–11.

Horner-Johnson, B.C., Gordon, R.G., 2010. True polar wander since 32 Ma B.P.: a paleomagnetic investigation of the skewness of magnetic anomaly 12r on the Pacific plate. J. Geophys. Res. 115, 9101.
Hüsing, S.K., Cascella, A., Hilgen, F.J., Krijgsman, W., Kuiper, K.F., Turco, E., Wilson, D., 2010. Astrochronology of the Mediterranean Langhian between 15.29 and 14.17 Ma. Earth Planet. Sci. Lett. 290, 254–269.
King, J., Banerjee, S.K., Marvin, J., 1983. A new rock-magnetic approach to selecting sediments for geomagnetic paleointensity studies: application to paleointensity for the last 4000 years. J. Geophys. Res 88, 5911–5921.
Kirschvink, J.L., 1980. The least-squares line and plane and the analysis of palaeomagnetic data. Geophys. J. R. Astron. Soc. 62, 699–718.
Lanci, L., Pares, J., Channell, J.E.T., Kent, D.V., 2004. Miocene magnetostratigraphy from Equatorial Pacific sediments (ODP Site 1218, Leg 199). Earth Planet. Sci. Lett. 226, 207–224.
Lourens, L.J., Hilgen, F.J., Laskar, J., Shackleton, N.J., Wilson, D., 2004. The Neogene period. In: Gradstein, F., Ogg, J., Smith, A. (Eds.), A Geological Time Scale. Cambridge University Press, pp. 409–440.
Lurcock, P.C., Wilson, G.S., 2012. PuffinPlot: a versatile, user-friendly program for paleomagnetic analysis. Geochem. Geophys. Geosyst. 13, Q06Z45, http://dx.doi.org/10.1029/2012GC004098.
Lyle, M., 2003. Neogene carbonate burial in the Pacific Ocean. Paleoceanography 18, 1–21.
Pälike, H., Lyle, M.W, Nishi, H., Raffi, I., Ridgwell, A., Gamage, K., Klaus, A., Acton, G., Anderson, L., Backman, J., Baldauf, J., Beltran, C., Bohaty, S.M., Bown, P., Busch, W., Channell, J.E.T., Chun, C.O.J., Delaney, M., Dewangan, P., Jones, T.D., Edgar, K. M., Evans, H., Fitch, P., Foster, G.L., Gussone, N., Hasegawa, H., Hathorne, E.C., Hayashi, H., Herrle, J.O., Holbourn, A., Hovan, S., Hyeong, K., Iijima, K., Ito, T., Kamikuri, S., Kimoto, K., Kuroda, J., Leon-Rodriguez, L., Malinverno, A., Moore Jr., T.C., Murphy, B.H., Murphy, D.P., Nakamura, H., Ogane, K., Ohneiser, C., Richter, C., Robinson, R., Rohling, E.J., Romero, O., Sawada, K., Scher, H., Schneider, L., Sluijs, A., Takata, H., Tian, J., Tsujimoto, A., Wade, B.S., Westerhold, T., Wilkens, R., Williams, T., Wilson, P.A., Yamamoto, Y., Yamamoto, S., Yamazaki, T., Zeebe, R. E., 2012. A Cenozoic record of the equatorial Pacific carbonate compensation depth. Nature 488, 609–614.
Pälike, H., Nishi, H., Lyle, M., Raffi, I., Klaus, A., Gamage, K., 2009. and the Expedition 320/321 Scientists, 2009. Pacific Equatorial Transect , IODP Preliminary Report, p. 320. http://dx.doi.org/10.2204/iodp.pr.320.2009.
Pälike, H., Norris, R.D., Herrle, J.O., Wilson, P.A., Coxall, H.K., Lear, C.H., Shackleton, N.J., Tripati, A.K., Wade, B.S., 2006. The heartbeat of the Oligocene climate system. Science 314, 1894–1898.
Pike, C.R., Roberts, A.P., Verosub, K.L., 1999. Characterizing interactions in fine magnetic particle systems using first order reversal curves. J. Appl. Phys. 85, 6660–6667.
Roberts, A.P., Pike, C.R., Verosub, K.L., 2000. First order reversal curve diagrams: a new tool for characterizing the magnetic properties of natural samples. J. Geophys. Res. 105, 28461–28475.
Schulz, M., Stattegger, K., 1997. Spectrum: spectral analysis of unevenly spaced paleoclimatic time series. Comput. Geosci. 23, 929–945.
Stoner, J.S., Channell, J.E.T., Hillaire-Marcel, C., 1995. Late Pleistocene relative geomagnetic paleointensity from deep Labrador Sea: regional and global correlations. Earth Planet. Sci. Lett. 134, 237–252.
Tauxe, L., 1993. Sedimentary records of relative paleointensity of the geomagnetic field: theory and practice. Rev. Geophys. 31, 319–354.
Tauxe, L., Hartl, P., 1997. 11 million years of Oligocene geomagnetic field behaviour. Geophys. J. Int. 128, 217–229.
Tauxe, L., 2006. Long-term trends in paleointensity: the contribution of DSDP/ODP submarine basaltic glass collections. Phys. Earth Planet. Inter. 156, 223–241.
Valet, J.P., Meynadier, L., 1993. Geomagnetic field intensity and reversals during the past four million years. Nature 366, 234–238.
Valet, J.P., Meynadier, L., Guyodo, Y., 2005. Geomagnetic dipole strength and reversal rate over the past two million years. Nature 435, 802–805.
Xuan, C., Channell, J.E.T., 2009. UPmag: MATLAB software for viewing and processing u channel or other pass-through paleomagnetic data. Geochem. Geophys. Geosyst. 10, 1–12 http://dx.doi.org/10.1029/2009GC002584.
Yamazaki, T., Oda, H.H., 2005. A geomagnetic paleointensity stack between 0.8 and 3.0 Ma from equatorial Pacific sediment cores. Geochem. Geophys. Geosyst. 6, Q11H20, http://dx.doi.org/10.1029/2005GC001001.
Zachos, J., Pagani, M., Sloan, L., Thomas, E., Billups, K., 2001a. Trends, rhythms, and aberrations in global climate 65 Ma to present. Science 292, 686–693.
Zachos, J.C., Shackleton, N.J., Revenaugh, J.S., Pälike, H., Flower, B.P., 2001b. Climate response to orbital forcing across the Oligocene–Miocene boundary. Science 292, 274–278.
Ziegler, L., Constable, C.G., Johnson, C.L., Tauxe, L., 2011. PADM2M: a penalized maximum likelihood model of the 0–2 Ma palaeomagnetic axial dipole moment. Geophys. J. Int. 184, 1069–1089.